Heliyon 6 (2020) e05359

Contents lists available at ScienceDirect

Heliyon

journal homepage: www.cell.com/heliyon

Research article

Contributions of protein microenvironment in tannase industrial applicability: An in-silico comparative study of pathogenic and non-pathogenic bacterial tannase

Ishita Biswas [a,1], Debanjan Mitra [a,1], Amal Kumar Bandyopadhyay [b,**], Pradeep K. Das Mohapatra [a,*]

[a] Department of Microbiology, Raiganj University, Raiganj, 733134, Uttar Dinajpur, West Bengal, India
[b] Department of Biotechnology, University of Burdwan, Burdwan, 713104, West Bengal, India

ARTICLE INFO

Keywords:
Biochemistry
Bioinformatics
Biotechnology
Microbiology
Molecular biology
Proteins
Tannase
Pathogenic and non-pathogenic bacteria
Salt bridge
Microenvironment
Order and disorder forming residues

ABSTRACT

Tannase is an inducible industrially important enzyme, produced by several microorganisms. A large number of bacteria have reported as tannase producers; however, some of them are pathogenic in nature. Therefore, it is quite uncertain whether the application of these tannase enzymes from such pathogenic bacteria is suitable for industries and human welfare. Till date, there is no clear evidence regarding which group of bacteria (non-pathogenic or pathogenic) is better suited for their application in the edge of industries with particular reference to the food industry. The present study is following the findings of the above queries. In this study, a large number of tannase protein sequences have been retrieved from the databases, including both non-pathogenic and pathogenic bacterial species. Physiochemical and evolutionary properties of those sequences have been evaluated. Results have shown that non-pathogenic bacterial tannase possesses a high number of acidic and basic amino acid residues as compared to their pathogenic counterparts. The acidic and basic amino acid residues of tannase provide unique microenvironment to it. In the other hand, the numbers of disorder forming residues are higher in tannase sequences of pathogenic bacteria. The study of tannase microenvironment leads in the formation of salt bridges, which finally favoring the stability and proper functioning of tannase. This is the first report of such observation on tannase enzyme using *in silico* approach. Study of the microenvironment concept will be helpful in protein engineering.

1. Introduction

Tannase (tannin acyl hydrolase, EC 3.1.1.20) is an extracellular inducible enzyme that catalyzes the hydrolysis of ester and depside bonds of several substrates such as gallotannins, epigallocatechin-3-gallate, esters of gallic acid, and epicatechin gallate and produces glucose and gallic acid as by-products (Mohapatra et al., 2005; Natarajan and Rajendran, 2012; Jana et al., 2014). The enzyme produced from microbial sources has immense applications in various industries due to its stability (Natarajan and Rajendran, 2012; Jana et al., 2014). Tannase is produced in the presence of tannic acid by different tannase producers including a large number of filamentous fungi such as *Aspergillus* sp. (Sharma et al., 2007), *Penicillium* sp. (Batra and Saxena, 2005), a massive number of bacteria (Mondal and Pati, 2000; Mohapatra et al., 2009) and few yeasts such as *Aureobasidium* sp. (Zhang et al., 2019), *Sporidiobolus* sp. (Kanpiengjai et al., 2020) and others. There are several reports in the literature on the bacterial origin of tannase. Lewis and Starkey (1969) first reported that *Achromobacter* sp. able to utilize gallotannin as the energy source for its growth. Deschamps et al. (1980) isolated several bacterial strains that can use tannic acid as the sole carbon source. Mondal and Pati (2000) reported on extracellular tannase production by newly isolated *Bacillus licheniformis* KBR6. Jana et al. (2013) have characterized thermostable tannase from *Bacillus subtilis* PAB2. High tannase activity has reported in *Lactobacillus Plantarum,* a lactic acid bacterium (Jiménez et al., 2014; Matsuda et al., 2016). Characterization of tannase activity in cell-free

* Corresponding author.
** Corresponding author.
E-mail addresses: akbanerjee@biotech.buruniv.ac.in (A.K. Bandyopadhyay), pkdmvu@gmail.com (P.K. Das Mohapatra).
[1] Both authors contributed equally.

https://doi.org/10.1016/j.heliyon.2020.e05359
Received 16 May 2020; Received in revised form 22 June 2020; Accepted 23 October 2020

extracts of *Lactobacillus plantarum* CECT 748T was performed by Rodriguez et al. (2008). Raghuwanshi et al. (2011) reported about highest tannase producer *Bacillus sphaericus* with potential gallic acid synthesis ability. Ren et al. (2013) first reported the crystal structure of a tannase from the bacterium *L. plantarum*. Comparative study of tannase from three closely related lactobacillus species such as *L. plantarum*, *L. paraplantarum*, and *L. pentosus* was conducted by Ueda et al. (2014). Kanpiengjaia et al. (2019) have isolated a new alkaline tannase from *Lactobacillus pentosus*. Jiménez et al. (2014) have reported the results of cloning and expression of the gene encoding TanSg1 tannase in *E. coli* from *Streptococcus gallolyticus* UCN34.

Tannase belongs to the enzyme class "hydrolase" and is one of the essential industrial enzymes (Jana et al., 2013). It has immense potential applications in several industrial sectors, including food, beverages, leather, chemical, pharmaceutical, and dye-making (Cavalcanti et al., 2020). It is extensively used for industrial effluent treatment and is also involved in the synthesis of gallic acid, instant tea (Hae-Soo et al., 2020; Unban et al., 2020; Thiyonila et al., 2020), acorn wine and coffee-flavoured soft drinks (Kar and Banerjee, 2000; Mohapatra et al., 2006; Jana et al., 2013). The enzyme also acts as a clarifier in the production of beer, fruit juices and to treat wastewater contaminated with polyphenolic compounds (Mohapatra et al., 2006; Sharma et al., 2007). It also involved in ripening of fruits (Jana et al., 2014) and wine production (Aracri et al., 2019).

Gallic acid, the hydrolysis product of tannic acid, is an antioxidant. It is a phenolic compound used in dye making, leather industry, as a photographic developer, pharmaceuticals for the synthesis of an antifolic and antibiotic drug - trimethoprim and in the production of pyrogallol (Mohapatra et al., 2005; Patil et al., 2011). It is also reported to suppress activation of proinflammatory and prooxidant gene expression induced by hyperglycemia (Kuppan et al., 2010).

Pyrogallol produced from gallic acid also has several industrial importances, like in coloring of hair, staining of fur, leathers and also in the preparation of anti-tumor and anti-cancer drugs (Jana et al., 2013).

The present study is concerned with the *in Silico* comparison of both non-pathogenic and pathogenic bacterial tannase and to answer about their safe application at industrial level.

2. Material and methods

2.1. Dataset

A detailed analysis of the sequence and structure of bacterial tannase was performed. A total 309 bacterial tannase sequences were retrieved from the UNIPROT database (UniProt: a hub for protein information, 2015). These sequences were divided in two groups-pathogenic and non-pathogenic bacteria tannase. These pathogenic bacteria were again divided into 4 subgroups - animal pathogens, human pathogen, plant pathogen, and both animal and plant pathogen based on their previous pathogenic reports (Hildebrand, 1971; Centurion-Lara et al., 1997; Podschun and Ullmann, 1998; Pauleta et al., 2001; Qin et al., 2011; Schröttner et al., 2014; Drancourt et al., 1997; Yadav et al., 2018; Kikuchi et al., 2020). Structures of non-pathogenic bacteria (*Lactobacillus plantarum*) were retrieved from the RCSB protein database (PDB) (Berman et al., 2000). Due to the lack of structure of pathogenic bacterial tannase, a model structure was created.

2.2. Multiple sequence alignment (MSA)

Multiple sequence alignment (MSA) was performed for all sequences using CLUSTAL Omega (Sievers et al., 2011) and the result was represented by JALVIEW (Clamp et al., 2004).

2.3. Physicochemical and evolutionary properties

Result of MSA was divided into two categories-block and non-block of sequences. Block of the sequence was prepared by BLOCK by using BLOCK MAKER (Henikoff et al., 1995). In BLOCK format all homologous positions are fixed. Each position may contain various kinds of residues. Both non block and block sequences were analysed by PHYSICO2 (Banerjee et al., 2015) for the calculation of physicochemical properties. It gives more than 20 types of residue level analysis and 46 window dependent properties form a protein FASTA file. Physicochemical parameters like amino acid compositions, GRAVY (grand average of hydropathy), pI, aliphatic index, disordered forming residues and ordered forming residues etc were calculated by the help of PHYSICO2. Based on the strength of order formation C, F, Y and W are taken as strong order forming residues. On the other hand, disorder regions of proteins were found to have higher content of R, E, G, Q, S, K. P and G. Most disorder residues based on their abundance in these proteins are R, E, S and P (Lieutaud et al., 2016) called disorder forming residues. Mean relative abundance (MRA) of sequences were calculated from the mean value of nonpathogenic bacterial tannase relative to pathogenic bacterial tannase to compare the data. Evolutionary properties of the sequences were calculated by the help of APBEST (Gupta et al., 2017). The phylogenetic tree was constructed by Figtree (Rambaut, 2014).

$$MRA = \frac{Mean\ value\ of\ non\ pathogenic\ bacterial\ tannase - Mean\ value\ of\ pathogenic\ bacterial\ tannase}{Mean\ value\ of\ pathogenic\ bacterial\ tannase}$$

2.4. Profile or signature detection for sequences

Identification of tannase protein family was previously performed (Banerjee et al., 2012). Protein profiles or signature site of all sequence were identified by PROSITE (Hulo et al., 2006).

2.5. Construction of model

Due to the lack of structure of pathogenic bacterial tannase, it was necessary to create a model. To make model of a protein, at least 30% similarity was crucial between target and template sequence. *Treponema* sp. (A0A353SAZ4) was used as a target which is a human pathogen. It shows highest sequence similarity with the template sequence. *Lactobacillus plantarum* (4J0K) was used as a template. The other structures of human pathogen showed less sequence similarity than *Treponema* sp. with that template structure. The model was developed by MODELLER V.1.1 (Fiser and Šali, 2003) and verified by Verify3d (Eisenberg et al., 1997) and Procheck (Laskowski et al., 1993).

2.6. Structural analysis

All structures were minimized in 1000 steps by using AUTOMINV.1 (Islam et al., 2018). Salt bridges were extracted with the help of SBION2 (Gupta et al., 2015). From this program, we got the number, types (isolated and network) and the position of salt bridges. The energy of those salt bridges was calculated by ADSBET2 (Nayek et al., 2015) (in case of the isolated salt bridge) and NUM (Bandyopadhyay et al., 2019b) (in case

Table 1. The type of pathogenicity, species name (sp.), accession number (ACC NO.), Disorder forming residues (DFR), Order forming residues (OFR), Grand average hydrophobicity (GRAVY), Isoelectric point (pI), Aliphatic index (Ali Ind) of tannase sequences.

Pathogenecity	Organism	ACC No.	DFR	OFR	GRAVY	pI	Ali Ind
animal infections	*Afipia broomeae*	A0A2M8ZGL7	23.8	11.2	-0.07	9.18	58.62
	Alteromonas sp.	A0A3D0T3E3	17.5	15	-0.19	5.62	53.62
human infections	*Aureimonas* sp.	A0A0N7KYJ3	17.5	8.8	-0.29	4.76	102.38
	Klebsiella sp.	A0A263JYJ0	13.8	11.2	-0.21	6.58	69.62
		A0A367NI18	22.5	11.2	-0.14	5.86	84.12
		A0A223UHG3	21.2	11.2	-0.20	7.43	80.50
		A0A443X042	22.5	10	0.07	8.7	90.38
	Serratia sp.	A0A2V1HI92	18.8	8.8	-0.33	6.59	108.38
	Burkholderia pyrrocinia	A0A318IM73	13.8	11.2	-0.24	8.46	86.62
		A0A318IRA2	20	12.5	-0.27	6.42	69.62
	Treponema sp.	A0A353SAZ4	18.8	8.8	-0.33	6.59	105.38
	Olsenella sp.	A0A356G5K5	18.4	8.8	-0.32	6.7	106.38
	Prolixibacteraceae bacteria	A0A3D1L1M7	18.8	8.8	-0.07	4.66	89.00
	Treponema sp.	A0A3D3FKB1	17.5	12.50	-0.27	6.44	85.38
	Comamonadaceae bacteria	A0A257EFG4	16.2	8.80	-0.09	5.11	94.00
	Paracoccus pantotrophus	A0A495PRV1	21.2	7.50	-0.24	5.57	106.25
	Actinomadura pelletieri	A0A495QG59	25	12.05	-0.08	10.0	79.12
	Burkholderia insecticola	R4WGR8	20.00	11.20	-0.3	6.01	96.25
plant pathogen	*Acidovorax delafieldii*	A0A165LSJ6	15.00	10	-0.1	5.05	84.38
		A0A168F6C6	17.5	11.2	-0.13	5.68	73.25
	Burkholderiales bacteria	A0A257CDD3	23.8	12.5	-0.19	5.58	85.25
		A0A257CF44	17.5	10	-0.21	4.99	90.25
		A0A257LE10	18.8	10	-0.19	5.69	90.38
		A0A257LKY7	17.5	11.2	-0.15	6.7	90.25
		A0A257LMN4	18.8	11.2	-0.19	8.57	70.88
		A0A257LQ11	17.5	8.8	-0.13	7.52	93.88
		A0A257LS17	12.5	11.2	-0.15	7.42	79.38
		A0A2G6TTL6	18.8	10	-0.13	8.47	82.88
	Acidovorax delafieldii	A0A2G6S9K8	15	12.5	-0.2	6.43	80.62
		A0A2G6SEL6	15	11.2	-0.06	5.77	80.75
		A0A2G6SF93	15	11.2	-0.29	6.7	79.38
		A0A2G6SWZ2	16.2	12.5	-0.18	5.09	72.12
		A0A2G6T023	16.2	11.2	-0.15	5.79	86.75
		A0A2G6T3X4	15	11.2	-0.32	6.41	79.25
		A0A2G6T435	13.8	11.2	-0.28	6.7	78.12
		A0A2G6Y6P7	16.2	12.5	-0.18	5.09	72.12
		A0A2G6Y9L4	16.2	11.2	-0.15	5.79	86.75
		A0A2G6YD70	13.8	11.2	-0.32	6.41	78.12
		A0A2G6YFP4	13.8	11.2	-0.27	6.7	76.88
		A0A2G6YFP8	17.5	11.2	-0.2	7.42	63.37
		A0A2M8X380	16.2	12.5	-0.2	6.43	81.88
		A0A2M8X900	15	11.2	-0.3	6.7	78.12
		A0A2T6JDP5	15	12.5	-0.2	6.43	79.38
		A0A2T6JI35	15	11.2	-0.3	6.7	78.12
		A0A2T6JIS1	17.5	11.2	-0.04	5.81	77
		A0A2U1DUF3	15	11.2	-0.3	6.7	78.12
		A0A2U1DV54	15	11.2	-0.06	5.77	80.75
		A0A2U1E0C9	15	12.5	-0.2	6.43	80.62
		A0A328ZHL3	18.8	10	-0.13	9.02	85.5
		A0A3D1MMR9	13.8	11.2	-0.29	6.86	72
		A0A3D1MP05	13.8	11.2	-0.18	7.42	74.37
		A0A3D1MU20	16.2	10	-0.04	5.81	78.25
		A0A3D1MUC9	15	12.5	-0.24	6.15	77
		A0A3L9YJ17	15	11.2	-0.06	5.77	80.75
		A0A3L9YPN5	15	11.2	-0.3	6.7	79.38
		A0A3L9YVD1	15	12.5	-0.2	6.43	80.62
		A0A495FGX1	15	11.2	-0.28	6.69	78.12
		A0A495FHM5	16.2	10	-0.04	5.81	78.25

(*continued on next page*)

Table 1 (*continued*)

Pathogenecity	Organism	ACC No.	DFR	OFR	GRAVY	pI	Ali Ind
		A0A495FIX7	13.8	11.2	-0.18	7.42	74.37
		A0A495I3C6	15	11.2	-0.29	6.86	78.12
		A0A495I3D2	13.8	11.2	-0.18	7.42	74.37
		A0A495I413	18.8	10	-0.03	5.84	77
		A0A497VBZ7	16.2	11.2	-0.15	5.79	86.75
		A0A497VC79	13.8	11.2	-0.29	6.7	83
		A0A497VGD2	15	11.2	-0.31	6.41	76.88
		A0A497VLT3	15	12.5	-0.19	5.09	73.38
	Actinophytocola oryzae	A0A4R7VHI7	15	13.8	-0.35	6.7	81.75
		A0A4R7W1F2	26.2	10	-0.1	7.62	91.5
	Xanthomonas translucens	A0A514EIB9	21.2	13.8	-0.33	5.84	79.25
	Acidovorax delafieldii	A0A543LJG9	17.5	11.2	-0.18	4.75	90.38
	Agrobacterium vitis	A0A560ZA01	13.8	13.8	-0.15	4.54	76.88
	Acidovorax delafieldii	A0A561XPS5	15	12.5	-0.2	6.43	80.62
		A0A561XT30	16.2	11.2	-0.06	5.81	80.75
		A0A561XTL3	15	11.2	-0.29	6.7	79.38
	Collimonas fungivorans	G0AEY7	23.8	11.2	-0.02	5.72	75.62
plants and animals	*Pseudomonas* sp.	A0A348R1P3	18.8	11.2	-0.14	4.84	80.5
		A0A348SKP4	21.2	11.2	-0.21	8.49	90.25
		A0A350ABK1	26.2	11.2	0.08	5.76	69.62
		A0A350ABR3	21.2	11.2	-0.22	8.5	90.25
		A0A350GWW1	26.2	10	0.07	7.63	82
		A0A350L0E4	21.2	11.2	-0.22	8.5	90.25
		A0A352G1I3	22.5	11.2	0.06	7.46	69.62
		A0A352HVP1	21.2	11.2	-0.22	8.5	90.25
		A0A355LIN0	18.8	11.2	-0.09	5.17	75.62
		A0A356N026	18.8	10	-0.21	7.59	90.25
		A0A357PTD1	25	11.2	0.07	5.76	69.62
		A0A358RT95	27	11.3	0.07	5.54	69.67
		A0A3B8SFW3	18.8	11.2	-0.09	5.17	75.62
		A0A3B8T8L2	26.2	11.2	0.08	5.76	69.62
		A0A3B9SB24	26.2	10	0.11	6.87	82
		A0A3B9TB99	26.4	10.1	0.12	6.88	80
		A0A3B9TL63	26.2	11.2	0.08	5.76	69.62
		A0A3C0PYC6	21.2	11.2	-0.22	8.5	90.25
		A0A3C1MPJ8	26.2	11.2	0.08	5.76	69.62
		A0A3C1MRL0	21.2	11.2	-0.22	8.5	90.25
		A0A3D0K9E4	22.5	11.2	-0.22	8.5	90.25
		A0A3D2DCS8	26.2	11.2	0.02	5.75	68.38
		A0A3D2M686	17.5	11.2	-0.12	4.84	75.62
		A0A3D2YCF8	21.2	11.2	-0.22	8.5	90.25
		A0A3D2YCU1	26.2	11.2	0.08	5.76	69.62
		A0A3D5QIX0	26.2	10	0.07	7.63	82
Average			18.5	11.1	-0.1565	6.55	81.088
Pathogenecity	Bacteria name	Acc No.	DFR	OFR	GRAVY	pI	Ali Ind
nonpathogenic	*Acidobacteria bacterium*	A0A1Q6XAT5	15.7	12.9	-0.26	5.08	69.86
		A0A1Q6YGT7	19	12.9	-0.22	5.08	67
		A0A1Q7CDI1	15.7	12.9	-0.3	4.72	69.86
		A0A1Q7FYN8	19.9	12.9	-0.16	6.44	79.57
		A0A1Q7GRJ8	15.3	11.4	-0.04	5.64	71.14
		A0A1Q7JGR3	17	12.9	-0.23	4.66	86.57
		A0A1Q7N8E5	20.7	12.9	-0.18	5.16	83.71
		A0A1Q7RTU7	19.9	12.9	-0.16	6.44	79.57
		A0A1Q8B829	18.4	12.9	-0.2	7.42	79.57
		A0A3D4FST8	15.7	11.4	-0.47	6.69	94.86
		A0A3D4FV49	20.7	11.4	0.04	6.45	68.29
		A0A3D4FXS1	15.7	12.9	-0.37	6.85	72.71
	Algoriphagus antarcticus	A0A3E0DS07	11.4	17.1	-0.51	6.13	91.86
	Aquitalea magnusonii	A0A3G9GHC6	12.9	11.4	-0.25	5.51	89.29

(*continued on next page*)

Table 1 (*continued*)

Pathogenecity	Organism	ACC No.	DFR	OFR	GRAVY	pI	Ali Ind
	Bacillus megaterium	A0A2A8SXE9	18.6	12.9	-0.09	6.71	80.86
		A0A2A8W381	18.6	12.9	-0.09	6.71	80.86
		A0A2A8W3A4	17.1	12.9	-0.07	10.1	71.14
		A0A2A9Y0I8	17.1	12.9	-0.09	10.1	69.71
		A0A2A9Y602	18.6	14.3	-0.12	6.44	80.86
		A0A5B8Q4C2	17.1	12.9	-0.13	7.56	80.86
		A0A5B8QEF4	17.1	12.9	-0.07	10.1	71.14
	Bradyrhizobium huanghuaihaiense	A0A562R4X4	17.1	10	-0.17	6.69	82.29
		A0A562R517	15.7	18.6	-0.31	9.54	82.29
		A0A562RG89	15.7	12.9	-0.44	4.41	86.43
	Bradyrhizobium lablabi	A0A2H9V655	18.4	10	-0.19	5.87	100.43
		A0A2H9VC52	14.3	12.9	-0.45	4.19	96.29
		A0A2H9VGU1	18.6	12.9	-0.01	5.68	78.29
		A0A2H9VHC6	12.9	12.9	-0.57	8.35	106
		A0A2H9VIF2	11.4	12.9	-0.31	6.42	90.57
	Brevundimonas diminuta	A0A246KNG1	18.9	11.4	-0.07	8.5	83.57
	Brevundimonas sp.	A0A2S8WC05	12.9	11.4	-0.23	8.49	76.86
	Bryobacterales bacteria	A0A3D1B235	14.3	14.3	-0.38	5.53	82.57
	Collimonas pratensis	A0A127PZK5	12.9	17.1	-0.36	6.41	88
		A0A127QSE8	11.4	17.1	-0.35	6.41	85.29
	Cyanobacteria bacteria	A0A350XI46	15	14.3	-0.31	7.4	92.14
	Dyadobacter jiangsuensis	A0A2P8GI72	14.3	11.4	-0.21	7.26	75.43
	Edaphobacter aggregans	A0A3R9PWC6	14.3	17.1	-0.4	7.42	81
	Edaphobacter dinghuensis	A0A495BU19	15.7	12.9	-0.38	7.42	96.14
	Edaphobacter modestus	A0A4Q7YT20	10	14.3	-0.4	6.42	80.86
		A0A4Q7YX34	12.9	11.4	-0.42	8.54	74
		A0A4Q7YXP6	20.3	14.3	-0.06	4.35	72.71
	Geodermatophilus tzadiensis	A0A2T0TQP9	12.9	12.9	-0.35	4.93	80.86
	Granulicella sp.	A0A3N1JX58	12.9	14.3	-0.29	5.64	85.29
	Herbaspirillum seropedicae	A0A4R8NQC9	17.1	12.9	-0.13	4.49	75.57
	Hydrogenophaga sp.	A0A350SR60	11.4	12.9	-0.32	9.06	82.43
		A0A350SZD1	14.3	15.7	-0.46	8.43	87.86
	Hylemonella gracilis	F3KUL5	17.1	12.9	-0.34	5.72	82.29
	Janthinobacterium sp.	A0A2M8YCU4	20.7	12.9	-0.06	7.42	83.86
	Komagataeibacter xylinus	A0A2D3HEP9	17.1	14.3	-0.42	4.65	76.71
		A0A2D3HIF4	15.7	11.4	-0.16	5.53	83.71
		A0A318PHP4	18.6	14.3	-0.4	4.65	76.71
	Kribbella sp.	A0A4Q7W028	10	12.9	-0.53	4.32	106
		A0A4R1WPV4	14.3	12.9	-0.21	4.64	89.14
		A0A4R1WQ69	18.6	14.3	-0.12	10.3	81
		A0A4R2CIW1	15	15.7	-0.17	10.2	75.43
		A0A4V2FE75	15	17.1	-0.26	9.48	83.71
	Kutzneria buriramensis	A0A3E0HZA0	8.6	11.4	-0.17	4.88	79.57
	Lactobacillus acidophilus	A0A448F3E0	15	11.4	-0.07	9.74	57.43
	Lactobacillus alimentarius	A0A2K9HQ50	15.7	14.3	-0.31	8.99	75.29
	Lactobacillus brevis	A0A3B8ETC4	17.1	17.1	-0.34	9.82	87.71
	Lactobacillus collinoides	A0A0R2BA86	11.4	11.4	-0.21	10.2	58.86
		A0A161XSA7	11.4	11.4	-0.21	10.2	58.86
	Lactobacillus curieae	A0A1S6QIR3	17.1	12.9	0.02	10.5	56
	Lactobacillus fabifermentans	A0A0R2NRK2	11.4	14.3	-0.39	9.27	68.43
		W6T5V7	11.4	14.3	-0.4	9.27	72.57
	Lactobacillus gasseri	A0A1V3Y4K2	15	11.4	-0.07	9.74	57.43
	Lactobacillus gastricus	A0A0R1V835	18.6	15.7	-0.28	6.42	81.14
	Lactobacillus namurensis	A0A0R1K9A6	17.1	11.4	-0.14	10.7	65.86
	Lactobacillus parabrevis	A0A0R1H2G9	17.1	15.7	-0.36	8.67	83.57
	Lactobacillus paracollinoides	A0A0R1TM22	11.4	11.4	-0.23	10.2	67.14
	Lactobacillus paragasseri	A0A558K1G1	15	11.4	-0.11	9.55	57.43
	Lactobacillus paraplantarum	A0A199QAR2	14.3	12.9	-0.3	8.63	75.29
		A0A2I9CLW7	12.9	12.9	-0.18	6.48	72.43

(*continued on next page*)

Table 1 (*continued*)

Pathogenecity	Organism	ACC No.	DFR	OFR	GRAVY	pI	Ali Ind
		A0A370A650	14.3	12.9	-0.25	4.72	79.43
		A0A4Q9XZC9	12.9	12.9	-0.18	6.48	72.43
		M5B2V9	14.3	12.9	-0.19	6.48	79.43
		T2HND3	12.9	12.9	-0.18	6.48	72.43
		T2HNE6	14.3	12.9	-0.18	6.48	78
		T2HNW8	14.3	12.9	-0.19	6.48	79.43
		T2HQX7	12.9	12.9	-0.13	4.8	72.43
	Lactobacillus paucivorans	A0A0R2LXK0	17.1	15.7	-0.36	9.92	80.71
	Lactobacillus pentosus	A0A2K9HZY9	12.9	15.7	-0.23	4.42	75.14
		A0A2K9I2I6	15.7	12.9	-0.22	10.4	58.86
		A0A2P1JP46	15.7	14.3	-0.18	4.5	71
		A0A2P1JP47	12.9	15.7	-0.24	4.72	71
		A0A2P1JP53	11.4	15.7	-0.32	4.33	78
		A0A2P1JP57	12.9	15.7	-0.25	4.72	72.43
		A0A2P1JP59	11.4	15.7	-0.3	4.71	72.43
		A0A2P1JP60	14.3	14.3	-0.19	4.42	72.43
		A0A2P1JP62	12.9	15.7	-0.25	4.72	72.43
		A0A2P1JP63	11.4	15.7	-0.26	4.42	72.43
		A0A2P1JP64	11.4	15.7	-0.3	4.71	73.86
		A0A2P1JP65	14.3	12.9	-0.16	4.42	72.43
		A0A2P1JP66	14.3	14.3	-0.19	4.42	72.43
		A0A2P1JP67	12.9	15.7	-0.25	4.72	72.43
		A0A2P1JP68	11.4	15.7	-0.3	4.71	72.43
		A0A2P1JP70	14.3	17.1	-0.35	4.33	79.43
		A0A2P1JP71	12.9	15.7	-0.25	4.72	72.43
		A0A2P1JP73	11.4	15.7	-0.3	4.71	72.43
		A0A2P1JP74	12.9	15.7	-0.25	4.72	72.43
		A0A2P1JP75	12.9	15.7	-0.25	4.72	72.43
		A0A2P1JP76	14.3	14.3	-0.21	4.42	75.14
		A0A2P1JP77	12.9	15.7	-0.25	4.72	72.43
		A0A2P1JP78	12.9	15.7	-0.25	4.72	72.43
		A0A2P1JP79	15.7	12.9	-0.15	4.42	71
		A0A2P1JP80	12.9	15.7	-0.25	4.72	72.43
		A0A2P1JP81	12.9	18.6	-0.3	6.45	73.86
		A0A2P1JP82	14.3	14.3	-0.19	4.42	72.43
		A0A2P1JP84	12.9	15.7	-0.25	4.72	72.43
		A0A2P1JP85	15.7	14.3	-0.19	4.42	72.43
		A0A2P1JP89	12.9	15.7	-0.25	4.72	72.43
		A0A2P1JP90	12.9	15.7	-0.25	4.72	72.43
		A0A2P1JP91	12.9	15.7	-0.25	4.72	72.43
		A0A2S9VNQ5	15.7	12.9	-0.22	10.4	58.86
		A0A2S9VVG1	14.3	14.3	-0.18	4.42	68.29
		A0A2S9VVX6	15.7	12.9	-0.22	10.4	58.86
		A0A2S9VXR8	14.3	14.3	-0.23	4.72	72.43
		A0A2S9VYM2	15.7	12.9	-0.22	10.4	58.86
		A0A2S9W5G2	15.7	14.3	-0.2	4.5	73.71
		A0A3M6KJL4	15.7	12.9	-0.22	10.4	58.86
		A0A3M6LNU9	12.9	15.7	-0.25	4.72	72.43
		A0A451G2X2	12.9	15.7	-0.25	5.62	71
		A0A494S5U8	15.7	12.9	-0.22	10.4	58.86
		F6IRL4	15.7	12.9	-0.22	10.4	58.86
		F6IX48	11.4	15.7	-0.3	4.71	72.43
		G0M044	15.7	12.9	-0.22	10.4	58.86
		G0M5X6	14.3	14.3	-0.19	4.42	72.43
		I9KYI4	14.3	14.3	-0.23	4.72	71
		M5AP49	15.7	14.3	-0.2	4.5	73.71
		T2HN93	12.9	15.7	-0.25	4.72	72.43
		T2HN96	15.7	14.3	-0.1	4.18	71
		T2HNG4	15.7	14.3	-0.15	4.31	73.71

(*continued on next page*)

Table 1 (*continued*)

Pathogenecity	Organism	ACC No.	DFR	OFR	GRAVY	pI	Ali Ind
		T2HNG6	12.9	15.7	-0.25	4.72	72.43
		T2HNY5	15.7	14.3	-0.2	4.5	73.71
		T2HNY8	11.4	15.7	-0.3	4.71	72.43
		T2HQY9	15.7	14.3	-0.16	4.89	73.71
		T2HQZ2	12.9	15.7	-0.17	4.25	72.43
	Lactobacillus plantarum	A0A0F7GJK2	14.3	12.9	-0.3	8.63	75.29
		A0A0G9GPE8	15.7	12.9	-0.23	10.4	58.86
		A0A199QJQ2	14.3	12.9	-0.19	6.48	79.43
		A0A1E3KV81	15.7	12.9	-0.29	8.63	75.29
		A0A1S0RU34	14.3	12.9	-0.3	8.63	75.29
		A0A1W6NR26	15.7	12.9	-0.23	10.4	58.86
		A0A387DIN7	14.3	12.9	-0.3	8.63	75.29
		A0A3Q9DYE5	14.3	12.9	-0.3	8.63	75.29
		A0A3S9KSF0	14.3	12.9	-0.3	8.63	75.29
		A0A3S9KSF3	14.3	12.9	-0.3	8.63	75.29
		A0A3S9KSF4	14.3	12.9	-0.3	8.63	75.29
		A0A494S935	14.3	12.9	-0.3	8.63	75.29
		A0A5F0YDB8	15.7	12.9	-0.25	9.27	75.29
		B3Y018	14.3	12.9	-0.3	8.63	75.29
		B9A0W2	14.3	12.9	-0.3	8.63	75.29
		D7VBF4	15.7	12.9	-0.23	10.4	58.86
		F9US92	14.3	12.9	-0.3	8.63	75.29
		T2HN98	14.3	12.9	-0.3	8.63	75.29
		T2HNH1	14.3	12.9	-0.3	8.63	75.29
		T2HNZ3	14.3	12.9	-0.3	8.63	75.29
		T2HNZ8	14.3	12.9	-0.3	8.63	75.29
		T2HPE5	14.3	12.9	-0.3	8.63	75.29
		T2HQZ7	14.3	12.9	-0.3	8.63	75.29
		T5JWN1	12.9	15.7	-0.25	4.72	71
	Lactobacillus senmaizukei	A0A0R2DS70	15.7	15.7	-0.57	9.3	87.86
	Lactobacillus sp.	A0A3R8J7D4	18.6	12.9	-0.12	9.27	83.57
		A0A5D0D7A8	14.3	12.9	-0.3	8.63	75.29
	Lactobacillus spicheri	A0A0F3RR38	14.3	12.9	-0.2	10.6	61.71
	Lactobacillus suantsaii	A0A4Q0VIH3	17.1	11.4	-0.25	10.2	72.86
	Lactobacillus zymae	A0A0R1MZ09	14.3	12.9	-0.23	10.4	60.29
	Marinobacterium mangrovicola	A0A4R1G7Z5	15.7	8.6	-0.25	5.74	93.57
		A0A4R1G8V6	14.3	11.4	-0.29	5.66	86.43
		A0A4R1GE88	11.4	11.4	-0.39	4.8	104.57
	Massilia flava	A0A562PHV0	14.3	10	-0.15	5.74	78.29
		A0A562Q3C7	10	17.1	-0.49	6.69	75.29
		A0A344JGV1	14.3	14.3	-0.41	6.41	78
		A0A2M9AR92	14.3	8.6	-0.29	4.94	112.86
		A0A2M9BHU9	12.9	12.9	-0.32	5.66	76.86
	Nostoc sp.	A0A318ARQ6	17.1	12.9	-0.26	6.86	94.71
		A0A318B3V5	20.4	15.7	-0.2	9.17	68.57
		A0A318B5P1	17.1	12.9	-0.19	6.43	86.57
		A0A318BCP8	14.3	14.3	-0.25	7.25	71.57
		A0A318BI76	18.6	11.4	0.04	7.52	61.57
	Novosphingobium taihuense	A0A562JN73	15.7	12.9	-0.24	6.16	86.57
		A0A562JV15	19.9	14.3	-0.11	6.44	75.29
	Paraburkholderia sp	A0A495FPL1	18.4	11.4	-0.3	4.17	78.14
		A0A495G1V4	14.3	10	-0.21	5.74	86.57
		A0A495G633	10	14.3	-0.29	4.56	82.43
		A0A495SWF3	18.4	14.3	-0.12	4.15	68.43
		A0A495T4J4	17.1	15.7	-0.33	4.94	83.86
		A0A495T4W0	18.6	12.9	-0.04	6.16	80.86
		A0A495TPB8	15.7	15.7	-0.34	7.42	76.86
		A0A495TQA4	15.7	15.7	-0.11	8.42	67

(*continued on next page*)

Table 1 (*continued*)

Pathogenecity	Organism	ACC No.	DFR	OFR	GRAVY	pI	Ali Ind
		A0A495TR06	12.9	14.3	-0.22	4.62	90.57
		A0A495TUG7	14.3	10	-0.24	6.42	90.86
		A0A4R1J3Z6	14.3	14.3	-0.36	5.97	75.14
	Pseudomonas duriflava	A0A562Q7H4	12.9	12.9	-0.2	4.58	74.14
	Pseudomonas floridensis	A0A1X0N509	18.6	12.9	-0.27	7.4	93.57
	Pseudosporangium ferrugineum	A0A2T0SB96	17.1	12.9	-0.3	5.46	72.71
	Pseudoxanthomonas taiwanensis	A0A562E413	19.9	12.9	-0.46	4.51	93.57
	Roseibium hamelinense	A0A562STT3	18.4	10	-0.18	8.36	89.29
	Simplicispira sp.	A0A2U1C8G6	18.6	15.7	-0.17	5.09	79.71
	Umezawaea tangerina	A0A2T0SBY3	19.9	15.7	-0.09	7.3	71.14
		A0A2T0SU30	15.4	14.3	-0.25	9.17	88
	Variovorax sp.	A0A109D437	18.4	15.7	-0.23	8.47	84
		A0A125NU60	14.3	11.4	-0.29	5.55	81
		A0A2G6WT85	15.7	12.9	-0.27	9.05	100.43
		A0A2G6X5N6	14.3	20	-0.46	8.99	85
		A0A2G6X5T3	12.9	15.7	-0.28	4.88	86.57
		A0A2G6X7X3	14.3	11.4	-0.28	4.51	95
		A0A2G6XA91	15.7	8.6	-0.26	5.08	96.43
Average		14.9	13.6	-0.245	6.73	76.42	

of the network salt bridge). NUM is a new concept to calculate those energies of network salt bridges. The identification of salt bridges microenvironment residues and their energies were calculated by an in house automated method (Mitra et al., 2019). PDB2PQR v1.9.0 (Dolinsky et al., 2004) was used to generate the partial atomic charge (Q) and radius (R) with a force field, CHARMM22 (Buck et al., 2006). The Poisson-Boltzmann calculations were performed to determine atomic potentials with the help of APBS (Jurrus et al., 2018). The concept of the microenvironment is new in this field (Nayek et al., 2015).

3. Results and discussion

3.1. Physiochemical and evolutionary analysis

Physiochemical properties of all the bacterial sequences were individually evaluated. Some differences have been identified between pathogenic and non-pathogenic bacterial tannase sequences (Table 1). The number of disorder forming residue (S + E + P + R) and order forming residue (C + F + Y + W) are critical properties for a protein (Lieutaud et al., 2016). GRAVY indicates the hydrophobic and hydrophilic nature of the protein (Kaur and Pati, 2018).

By the analysis of physicochemical properties (Table 1), it showed that the tannase sequences of pathogenic bacteria contain high number of disorder forming residues, which means it can cause some diseases in human or create toxicity in enzymatic reaction (Tretyachenko et al., 2017). On the other hand, tannase sequences of non-pathogenic bacteria contain high number of order forming residue. The present study reveals that the negative value of GRAVY of non-pathogenic bacterial tannase indicates that it is hydrophilic in nature. It could easily mix with any aqueous medium (Schröder, 2017). Enzymes with less disorder forming residues and highly hydrophilic in nature are highly stable and are could be very helpful and profitable for industries (Rigoldi et al., 2018). The

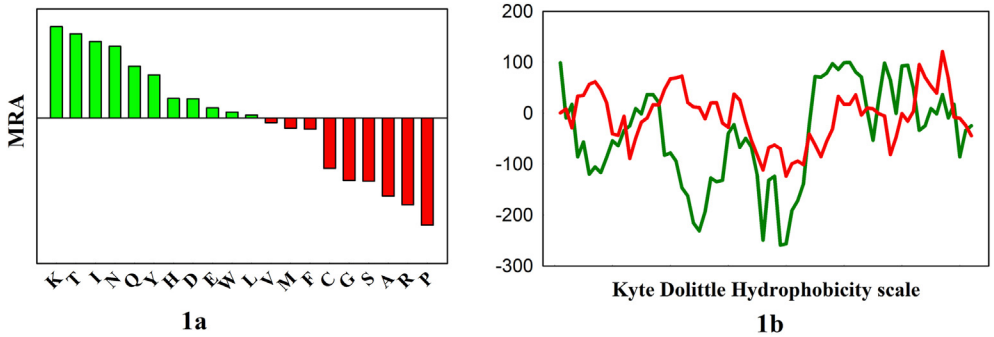

Figure 1. 1a.Mean relative abundance (MRA) of Amino acid composition of non-pathogenic sequence 1b. Kyte dolittle hydrophobicity scale of pathogenic (red line) and non-pathogenic (green line) bacterial tannase sequence.

Table 2. Evolutionary properties like maximum conserved residue (MCR), Maximum diverse residue (MDR), Dominant hetero pair (DHP), Non conserve and conserve ratio (R) and E value of non-pathogenic bacterial tannase and pathogenic bacterial tannase sequences.

Properties	Non pathogenic	Pathogenic
MCR	A > T > V	A > L > V
MDR	G > A > Y	G > A > D
DHP	AG > DV > EA	ML > SA > AG
R ratio	100.14	85.99
E value	65.98	57.68

Table 3. Type of organism with their site profile name and accession number in relation to tannase.

Type of organism	Site profile name	Acc. No.
Nonpathogenic	Eukaryotic thiol (cysteine) proteases histidine active site	A0A2P8GI72
	Glycoprotein hormones beta chain signature 1	A0A350XI46
		A0A2H9VHC6
	Prokaryotic membrane lipoprotein lipid attachment site profile	A0A2H9V655
		A0A2H9VIF2
		A0A2G6X5T3
		A0A125NU60
		A0A109D437
		A0A2G6WT85
		A0A2G6XA91
		A0A2G6X7X3
		A0A4R1G7Z5
		A0A495T4W0
		A0A495G1V4
		A0A495FPL1
		A0A3D4FV49
		A0A3D4FST8
		A0A0G9GPE8
		D7VBF4
		A0A1W6NR26
		A0A448F3E0
		A0A0R1TM22
		A0A558K1G1
		A0A1V3Y4K2
		A0A0R2BA86
		A0A161XSA7
		A0A0R1K9A6
		A0A0F3RR38
		F6IRL4
		G0M044
		A0A494S5U8
		A0A2K9I2I6
		A0A2S9VYM2
		A0A3M6KJL4
		A0A2S9VNQ5
		A0A2S9VVX6
		A0A4R8NQC9
		A0A127QSE8
		A0A127PZK5
	Twin arginine translocation (Tat) signal profile	A0A2T0TQP9
		A0A2H9VGU1
	Type-1 copper (blue) proteins signature	A0A3D4FWC6
	Zinc-containing alcohol dehydrogenases signature	A0A495T4J4
Human pathogen	Prokaryotic membrane lipoprotein lipid attachment site profile	A0A318IM73
		A0A353SAZ4
		A0A257FZW4
		A0A2V1HI92
	Serine/threonine dehydratases pyridoxal-phosphate attachment site	A0A495PRV1
	TonB-dependent receptor proteins signature 1	A0A3D3FKB1
	Twin arginine translocation (Tat) signal profile	A0A356G5K5
plant pathogen	Prokaryotic membrane lipoprotein lipid attachment site profile	A0A257LMN4
		A0A257LS17
		A0A2G6TTL6
		A0A257LKY7
		A0A514EIB9
		G0AEY7
		A0A168F6C6
		A0A2G6SEL6

(*continued on next page*)

Table 3 (*continued*)

Type of organism	Site profile name	Acc. No.
		A0A2G6YFP4
		A0A2T6JI35
		A0A495FHM5
		A0A2U1DUF3
		A0A497VC79
		A0A543LJG9
		A0A495I3D2
		A0A2G6T023
		A0A3L9YVD1
		A0A2G6SF93
		A0A2G6YD70
		A0A495FGX1
		A0A3L9YPN5
		A0A561XTL3
		A0A3D1MP05

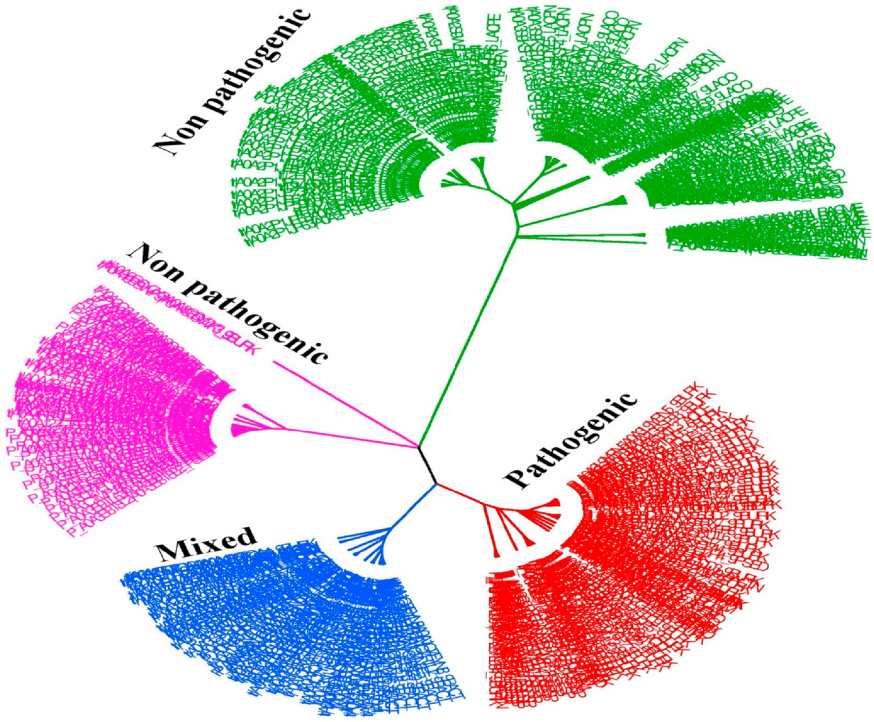

Figure 2. Phylogenetic tree showed relationship between non-pathogenic (green, pink) and pathogenic (red) bacterial tannase. A similar relation clade (blue) also found between them.

isoelectric point of non-pathogenic sequences is slightly higher than pathogenic bacterial tannase. The result of pI indicates that non-pathogenic bacterial tannase can tolerate a wide range of pH (Kiraga et al., 2007). The aliphatic index of the non-pathogenic and pathogenic bacterial tannase is almost equal. That means the thermal stability of those proteins is nearly the same (Panda and Chandra, 2012).

From the analysis of amino acid composition (Figure 1.) of two groups of bacterial tannase sequences, it is clear that high number of acidic and basic residues (except R) are present in non-pathogenic bacterial tannase. Hydrophobic amino acids showed higher abundance in pathogenic sequences. Kyte Dolittle hydrophobicity scale indicated that those non-pathogenic bacterial tannases are highly hydrophilic in nature (Figure 1b green line). It means it could easily interact with the liquid or aqueous medium which is beneficial for industrial applications (Schröder, 2017). On the other hand, those pathogenic bacterial tannase are hydrophobic in nature (Figure 1b red line).

Analysis of evolutionary properties of both groups of sequences (Table 2) have shown that the maximum conserve residues are almost same in both non-pathogenic and pathogenic bacterial tannases. In the case of the maximum diverse residue (MDR), it also showed almost identical residues except for the third one of pathogenic bacterial tannase. It is neutral polar in non-pathogenic bacterial tannase whereas it is acidic polar in pathogenic bacterial tannase. Charged residues positively affect the dominant hetero pair groups in non-pathogenic bacterial tannase. The R ratio, i.e. non conserve/conserve residue ratio is low in pathogenic bacterial tannase sequences. That means their divergence is strictly restricted (Bandyopadhyay et al., 2019a). E value, i.e. use of

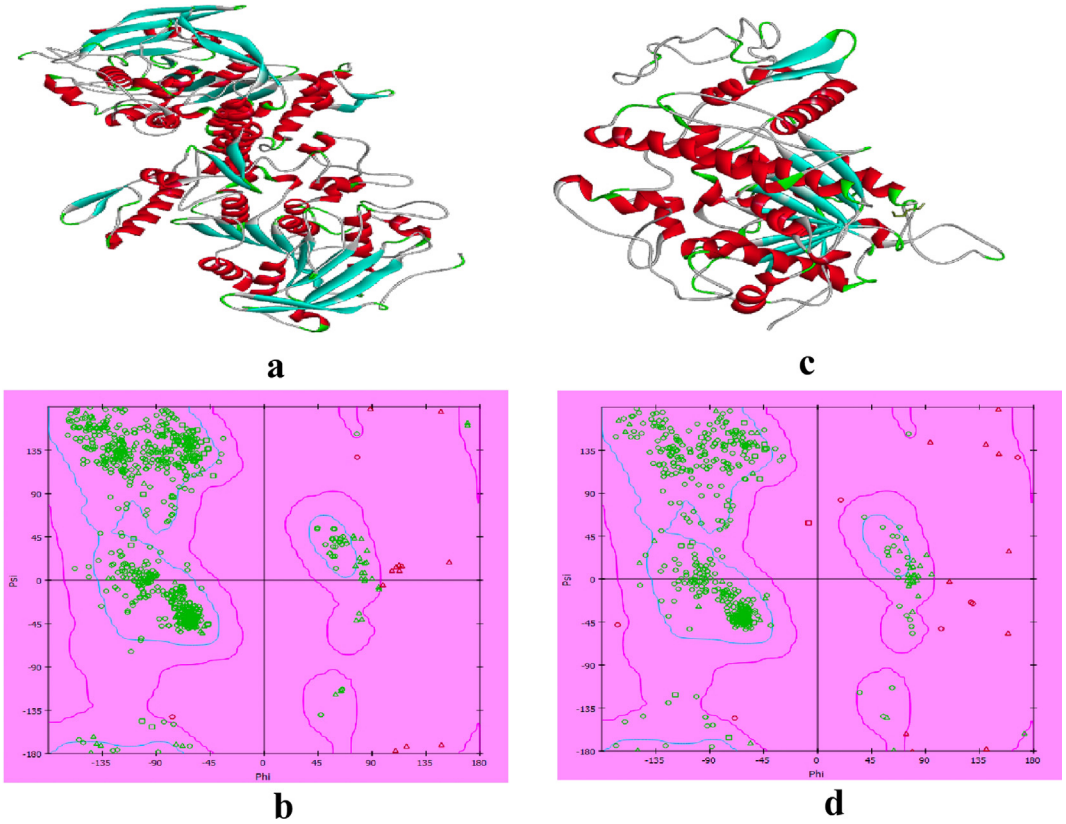

Figure 3. 3a showed the template protein 4J0K (both A and B chain) structure, 3b represented the Ramachandran plot of template protein (single chain), 3c showed the model structure of Treponema sp., 3d represented the Ramachandran plot of model protein.

dominant hetero pair is high in non-pathogenic bacterial tannase. That means they used their charged residues rigorously. So, the overall analysis of sequences of both groups indicates that acidic and basic residues have a principal role in non-pathogenic bacterial tannase sequences.

3.2. Conservation more in pathogenic bacterial tannase

The result of MSA showed that a large number of single conserve amino acid positions are present in pathogenic bacterial tannase. Conserved amino acid positions 193(G), 196(G), 231(G), 232(H), 314(Y), 317(G), 322(G), 323(R), 334(P), 362(G), 431(D), 484(C), 485(L), 643(K), 648(G), 652(D), 692(P), 693(G), 740(W), 741(E) were found in all pathogenic bacterial tannase. Most positions are prevalent by neutral non-polar amino acid Glycine. Conserved amino acids position number 196(P), 297(G), 298(Y), 432(G), 433(G), 932(H), 979(W) are found in non-pathogenic bacterial tannase. From the above result, it is found that single conserve amino acid positions are much higher in pathogenic bacterial tannase that support the R ratio value.

3.3. Similarity in site profile

Six types of site profile in non-pathogenic bacterial tannase and four types of site profile in pathogenic bacterial tannase have been identified (Table 3). Both types of bacterial tannase showed a common site profile which is prokaryotic membrane lipoprotein lipid attachment site profile. It was found in 36 sequences of non-pathogenic bacterial tannase and 23 sequences of pathogenic bacterial tannase. Twin arginine translocation

Table 4. Details of the Ramachandran plot of *Lactobacillus plantarum* (4J0K) and *Treponema* sp. (model).

Properties	Properties	*Lactobacillus plantarum* (PDB ID-4J0K)	*Treponema* sp. (model)
Plot area	residues in favored region	89.90%	82.90 %
	residues in allowed region	9.20%	13.40%
	residues in generously region	0.40%	1.50%
	residues in disallowed region	0.50%	2.20%
Residue properties	Max. deviation	19.9	7.7
	Bad contacts	0	0
G-factors	Dihedrals	-0.16	-0.43
	Covalent	-0.02	0.08
	Overall	-0.12	-0.27

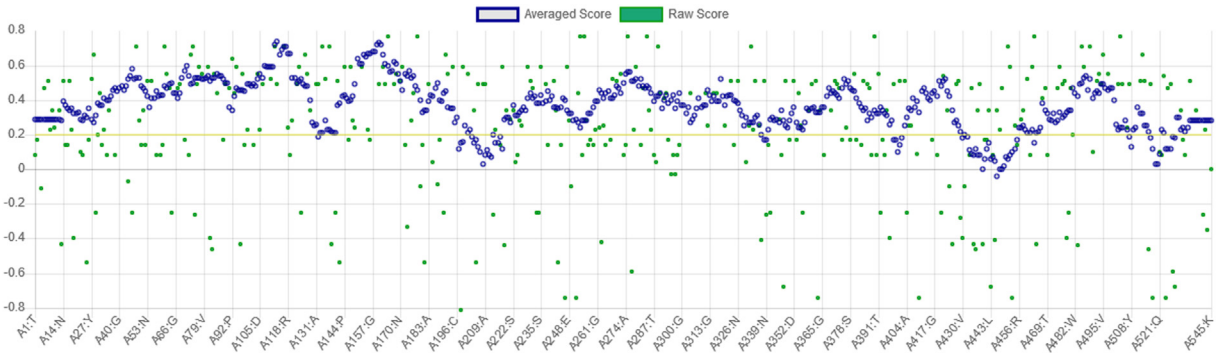

Figure 4. Average 3D-1D score of model structure of *Treponema* sp.

Table 5. No. of salt bridges (isolated and network) with desolvation (ΔΔGdslv), bridge (ΔΔGbrd), background (ΔΔGbac), total net energy (ΔΔGnet) of structures of *Lactobacillus plantarum* and model structure of non-pathogenic bacterial tannase.

Proteins name	No. of Isolated salt bridges	ΔΔGdslv (Kcal/mol)	ΔΔGbrd (Kcal/mol)	ΔΔGbac (Kcal/mol)	ΔΔGnet (Kcal/mol)
3WA6	9	99.95	-117.75	-25.45	-43.25
3WA7	9	97.57	-114.76	-27.13	-44.32
4J0C	9	100.01	-110.3	-36.16	-46.45
4J0D	11	121.95	-142.6	-40.92	-61.57
4J0G	8	81.82	-98.93	-35.21	-52.32
4J0H	8	96.13	-104.1	-38.43	-46.4
4J0I	10	121.24	-123.92	-49.53	-52.21
4J0J	10	124.53	-124.16	-49.29	-48.92
4J0K	12	122.84	-140.22	-50.6	-67.98
4JUI	10	119.36	-135.67	-45.37	-61.68
MODEL	11	97.64	-114.28	-12.25	-28.89
Proteins name	No. of Network salt bridges	ΔΔGdslv (Kcal/mol)	ΔΔGbrd (Kcal/mol)	ΔΔGbac (Kcal/mol)	ΔΔGnet (Kcal/mol)
3WA6	4	88.62	-117.46	-8.66	-37.5
3WA7	3	72.79	-99.31	-7.41	-33.99
4J0C	4	95.57	-133.87	-0.51	-38.8
4J0D	3	67.11	-91.91	-1.24	-26.04
4J0G	5	105.43	-141.32	-8.45	-44.37
4J0H	5	93.13	-130.3	-12.14	-49.31
4J0I	4	93.39	-125.08	-6.23	-37.93
4J0J	5	103.09	-148.2	-12.84	-57.96
4J0K	3	59.93	-79.31	-7.57	-26.97
4JUI	4	72.39	-101.29	-2.54	-31.46
MODEL	2	40.1	-54.88	-3.33	-18.1

(Tat) signal profile was also found in both groups of sequences. In case of non-pathogenic bacterial tannase, 4 types of signature specially found; Glycoprotein hormones beta chain signature 1, Eukaryotic thiol (cysteine) proteases histidine active site, Type-1 copper (blue) proteins signature and Zinc-containing alcohol dehydrogenases. Pathogenic bacterial tannase also possesses some unique sites like Serine/threonine dehydratases pyridoxal-phosphate attachment site, TonB-dependent receptor proteins signature 1.

3.4. Relationship between two groups

Phylogenetic group reveals the relation between non-pathogenic and pathogenic bacterial tannase (Figure 2.). Total 4 clades have been found. All the firmicutes (green) were found to form a big clade at one side of the Phylogenetic tree. This clade contains all species of *Lactobacillus*. The pink clade contains all non-pathogenic proteobacteria that produce tannase. All pathogenic bacteria has formed a different clade (red) at one side of the phylogenetic tree. The most exciting clade is blue clade which contained both pathogenic and non-pathogenic proteobacteria. It indicates that they had some sequence similarity. The decoration of branching in a phylogenetic tree demonstrates how those groups of tannase producing bacteria evolved from a series of familiar forbears.

3.5. Evaluation of model

After preparation, the model was evaluated by verify3D (Eisenberg et al., 1997) and Procheck (Laskowski et al., 1993) (Figure 3). Global Model Quality Estimation (GMQE) was showed 0.60, which indicated that it got higher reliability. In case of the Ramachandran plot, the model showed 82.90% in favored regions, 13.40 % in additional allowed regions, 1.50% in generously allowed regions (Table 4). It was almost similar to the template structure. The maximum deviation of the model structure was 7.7 and no bad contacts were found. The overall G-factors are negative, which indicates that it was a good model (Maheshwari and Jain, 2019). RMSD of the model with the template was

Table 6. Microenvironment residues with their number, types and their contributing energies of structures of *Lactobacillus plantarum* and model structure of non-pathogenic bacterial tannase.

Microenvironment residues of isolated salt bridges						
Proteins ID	Total number of microenvironment residues	Total energy of microenvironment Kj/mol	acid	base	neutral polar	hydrophobic
3WA6	69	-85.43	12	25	26	6
3WA7	68	-92.73	12	25	25	6
4J0C	64	-136.20	13	21	25	5
4J0D	92	-158.69	21	27	34	10
4J0G	57	-154.04	11	20	21	5
4J0H	66	-138.21	10	22	29	5
4J0I	84	-176.74	17	27	31	9
4J0J	89	-170.92	17	33	30	9
4J0K	88	-190.32	16	30	32	10
4JUI	83	-167.53	15	27	31	10
MODEL	68	-38.15	26	14	20	8
Microenvironment residues of network salt bridges						
Proteins ID	Total number of microenvironment residues	Total energy of microenvironment Kj/mol	Types of residues			
			acid	base	neutral polar	hydrophobic
3WA6	64	-50.81	16	18	19	11
3WA7	35	-43.10	8	7	14	6
4J0C	64	-15.81	17	17	19	11
4J0D	50	-17.73	12	14	15	9
4J0G	61	-34.19	19	18	15	9
4J0H	73	-61.46	20	22	19	12
4J0I	63	-38.48	18	17	17	11
4J0J	53	-68.15	15	14	15	9
4J0K	58	-42.96	19	16	14	9
4JUI	48	-21.73	13	15	13	7
MODEL	22	-13.25	8	6	6	2

1.7, that stated the folding pattern were same in both structures (Carugo, 2003).

The average 3D-1D score (Figure 4.) of that model structure of *Treponema* sp. showed >0.2 score and indicated that 94.14% residues had that score.

3.6. Proof of higher stability

All minimized structures of *Lactobacillus plantarum* (3WA6, 3WA7, 4J0C, 4J0D, 4J0G, 4J0H, 4J0I, 4J0J, 4J0K, 4JUI) and model structure of non-pathogenic bacterial tannase were minimized in 1000 steps for structural analysis. Both types of salt bridges, i.e. isolated and network salt bridges were analyzed.

In case of isolated salt bridges, structures of non-pathogenic bacterial tannase showed higher number of salt bridges than the pathogenic model structure (Table 5). 4J0K showed highest isolated salt bridge energies. Not only the number of salt bridges but also the energies per salt bridge are also higher in non-pathogenic bacterial tannase. Although the length of pathogenic bacterial tannase model structure (546 amino acids) is larger than those non-pathogenic bacterial tannase structures (470 amino acids), but the numbers of salt bridges are higher in non-pathogenic bacterial tannase structures due to high number of charged residues. In the case of network salt bridge, it is also found that higher salt bridge energy is present in non-pathogenic bacterial tannase than pathogenic bacterial tannase (Table 5). 4J0J showed highest network salt bridge energies among all those structures. These results indicated that non-pathogenic bacterial tannase showed higher stability in the extreme environment. In each type of salt bridges, the background energy always higher in non-pathogenic bacterial tannase, that indicates the background might have a role in providing stability of the protein. So the energy of those residues which act as microenvironments of salt bridges were identified and calculated. High numbers of salt bridges and their associated higher energy help the protein to stabilize in an extreme condition such as high temperature (Kumar and Nussinov 1999), high salt (Bandyopadhyay et al., 2019a) and high pH (Gallivan and Dougherty 2000). Salt bridge of protein can remain stable within an increased range of temperature (284–348K) (Belur and Mugeraya 2011). These salt bridges are surrounded by polar, charged and non-polar residues which have identified as microenvironment of salt bridges (Mitra et al., 2019). These residues affect the stability of proteins by contributing favorable or unfavorable environment.

3.7. Effect of intrinsic microenvironment

The microenvironment plays an excellent role in increasing the stability of the protein. The interaction of microenvironment residues and its partner salt bridge is equally likely neutral or favourable or unfavourable depending on the amino acid composition of the proteins.

Table 6 showed that the microenvironment residues of both types of salt bridges contribute high energies to increase the stability of non-pathogenic bacterial tannase than pathogenic bacterial tannase. 4J0K shows highest isolated salt bridge microenvironment energies whereas 4J0J shows highest network salt bridge microenvironment energies. It is also found that high number of residue involvement in the microenvironment of non-pathogenic bacterial tannase gives more stability. Charged residues play the leading role in forming of the microenvironment of salt bridges. Those charged residue does not constitute any salt bridges; instead, the protein used them as a microenvironment residue. Neutral polar residues also positively act as microenvironment of a salt bridge. The hydrophobic residues showed lower abundance in microenvironment residues. Some microenvironment residues contribute high energies in salt bridge stability. The unfavourable residues of microenvironments provide a clue for site-directed mutagenesis and help in protein engineering (Mitra et al., 2019). By changing a single

unfavourable microenvironment residue with a favourable one, the more stable structure will be created for industrial applications.

4. Conclusion

In silico study of bacterial tannase of non-pathogenic bacteria in comparison to pathogenic bacteria showed positive MRA of acidic and basic residues which alter the sequence property and not the structure. Due to the low number of disorder forming residues but high order forming residues and high hydrophilic nature of non-pathogenic bacterial tannase, it might be beneficial and safe for industrial purpose, especially in food industries. The acidic and basic residues also help in providing stability of the protein by forming salt bridges and favourable microenvironments. The statistical analysis of microenvironment residues of non-pathogenic bacterial tannase showed the importance in increasing the stability of tannase. By this study, we have identified the better tannase sources for industrial uses. Salt bridges and highly favourable microenvironment residue are very much important for the stability of the non-pathogenic bacterial tannase in the extreme environmental conditions. This is the first report where the effect of salt bridges and microenvironment residues in bacterial tannase have been reported. The concept of salt bridge's microenvironment is a novel concept in the field of structural biology.

Declarations

Author contribution statement

Ishita Biswas: Conceived and designed the experiments; Wrote the paper.

Debanjan Mitra: Conceived and designed the experiments; Performed the experiments; Analyzed and interpreted the data; Wrote the paper.

Amal Kumar Bandyopadhyay: Contributed analysis tools and interpreted the data.

Pradeep K. Das Mohapatra: Performed the experiments; Wrote the paper.

Funding statement

This research did not receive any specific grant from funding agencies in the public, commercial, or not-for-profit sectors.

Competing interest statement

The authors declare no conflict of interest.

Additional information

No additional information is available for this paper.

References

Aracri, F.M., Cavalcanti, R.M.F., Guimarães, L.H.S., 2019. Extracellular tannase from Aspergillus ochraceus: influence of the culture conditions on biofilm formation, enzyme production, and application. J. Microbiol. Biotechnol. 29, 1749–1759.

Bandyopadhyay, A.K., Islam, R.N.U., Mitra, D., Banerjee, S., Yasmeen, S., Goswami, A., 2019a. Insights from the salt bridge analysis of malate dehydrogenase from H. salinarum and E. coli. Bioinformation 15, 95.

Bandyopadhyay, A.K., Islam, R.N.U., Mitra, D., Banerjee, S., Goswami, A., 2019b. Stability of buried and networked salt-bridges (BNSB) in thermophilic proteins. Bioinformation 15, 61–67.

Banerjee, A., Jana, A., Pati, B.R., Mondal, K.C., Mohapatra, P.K.D., 2012. Characterization of tannase protein sequences of bacteria and fungi: an in silico study. Protein J. 31, 306–327.

Banerjee, S., Gupta, P.S.S., Nayek, A., Das, S., Sur, V.P., Seth, P., Islam, R.N.U., Bandyopadhyay, A.K., 2015. PHYSICO2: an UNIX based standalone procedure for computation of physicochemical, window-dependent and substitution based evolutionary properties of protein sequences along with automated block preparation tool, version 2. Bioinformation 11, 366–368.

Batra, A., Saxena, R.K., 2005. Potential tannase producers from the genera *Aspergillus* and *Penicillium*. Process Biochem. 40, 1553–1557.

Belur, P.D., Mugeraya, G., 2011. Microbial production of tannase: state of the art. Res. J. Microbiol. 6, 25–40.

Berman, H.M., Westbrook, J., Feng, Z., Gilliland, G., Bhat, T.N., Weissig, H., Shindyalov, I.N., Bourne, P.E., 2000. The protein data bank. Nucleic Acids Res. 28, 235–242.

Buck, M., Bouguet-Bonnet, S., Pastor, R.W., MacKerell Jr., A.D., 2006. Importance of the CMAP correction to the CHARMM22 protein force field: dynamics of hen lysozyme. Biophysics 90, L36–L38.

Carugo, O., 2003. How root-mean-square distance (rmsd) values depend on the resolution of protein structures that are compared. J. Appl. Cryst. 36, 125–128.

Cavalcanti, R.M.F., Martinez, M.L.L., Oliveira, W.P., Guimarães, L.H.S., 2020. Stabilization and application of spray-dried tannase from Aspergillus fumigatus CAS21 in the presence of different carriers. 3 Biotech 10, 1–14.

Centurion-Lara, A., Arroll, T., Castillo, R., Shaffer, J.M., Castro, C., Van Voorhis, W.C., Lukehart, S.A., 1997. Conservation of the 15-kilodalton lipoprotein among Treponema pallidum subspecies and strains and other pathogenic treponemes: genetic and antigenic analyses. Infect. Immun. 65, 1440–1444. PubMed -9119485.

Clamp, M., Cuff, J., Searle, S.M., Barton, G.J., 2004. The jalview java alignment editor. Bioinformatics 20, 426–427.

Dolinsky, T.J., Nielsen, J.E., McCammon, J.A., Baker, N.A., 2004. PDB2PQR: an automated pipeline for the setup of Poisson–Boltzmann electrostatics calculations. Nucleic Acids Res. 32, W665–W667.

Drancourt, M., Brouqui, P., Raoult, D., 1997. Afipia clevelandensis antibodies and cross-reactivity with Brucella spp. and Yersinia enterocolitica O: 9. Clin. Diagn. Lab. Immunol. 4, 748–752. PubMed: 9384302.

Eisenberg, D., Lüthy, R., Bowie, J.U., 1997. VERIFY3D: assessment of protein models with three-dimensional profiles. Methods Enzymol. 277, 396–404.

Fiser, A., Šali, A., 2003. Modeller: generation and refinement of homology-based protein structure models. Methods Enzymol. 374, 461–491.

Gallivan, J.P., Dougherty, D.A., 2000. A computational study of cation− π interactions vs salt bridges in aqueous media: implications for protein engineering. J. Am. Chem. Soc. 122, 870–874.

Gupta, P.S.S., Nayek, A., Banerjee, S., Seth, P., Das, S., Sur, V.P., Roy, C., Bandyopadhyay, A.K., 2015. SBION2: analyses of salt bridges from multiple structure files, version 2. Bioinformation 11, 39–42.

Gupta, P.S.S., Banerjee, S., Islam, R.N.U., Sur, V.P., Bandyopadhyay, A.K., 2017. Substitutional analysis of orthologous protein families using BLOCKS. Bioinformation 13 (1), 1–7. https://www.ncbi.nlm.nih.gov/pmc/articles/PMC5405086/.

Hae-Soo, K.I.M., Do Yeon, J.E.O.N., Javaid, H.M.A., Sahar, N.E., Ha-Nul, L.E.E., Seong-Jin, H.O.N.G., Young-Min, K.I.M., 2020. Bio-transformation of green tea infusion with tannase and its improvement on adipocyte metabolism. Enzym. Microb. Technol. 135, 109496.

Henikoff, S., Henikoff, J.G., Alford, W.J., Pietrokovski, S., 1995. Automated construction and graphical presentation of protein blocks from unaligned sequences. Gene 163, GC17–GC26.

Hildebrand, D.C., 1971. Pectate and pectin gels for differentiation of Pseudomonas sp. and other bacterial plant pathogens. Phytopathology 61.

Hulo, N., Bairoch, A., Bulliard, V., Cerutti, L., De Castro, E., Langendijk-Genevaux, P.S., Pagni, M., Sigrist, C.J., 2006. The PROSITE database. Nucleic Acids Res. 34, D227–D230.

Islam, R.N.U., Mitra, D., Gupta, P.S.S., Banerjee, S., Mondal, B., Bandyopadhyay, A.K., 2018. AUTOMINv1. 0: an automation for minimization of Protein Data Bank files and its usage. Bioinformation 14, 525–529.

Jana, A., Maity, C., Halder, S.K., Das, A., Pati, B.R., Mondal, K.C., Mohapatra, P.K.D., 2013. Structural characterization of thermostable, solvent tolerant, cytosafe tannase from Bacillus subtilis PAB2. Biochem. Eng. J. 77, 161–170.

Jana, A., Halder, S.K., Banerjee, A., Paul, T., Pati, B.R., Mondal, K.C., 2014. Biosynthesis, structural architecture and biotechnological potential of bacterial tannase: a molecular advancement. Bioresour. Technol. 157, 327–340.

Jiménez, N., Barcenilla, J.M., López de Felipe, F., de las Rivas, B., Muñoz, R., 2014. Characterization of a bacterial tannase from Streptococcus gallolyticus UCN34 suitable for tannin biodegradation. Appl. Microbiol. Biotechnol. 98, 6329–6337.

Jiménez, N., Esteban-Torres, M., Mancheño, J.M., de las Rivas, B., Muñoza, R., 2014. Tannin degradation by a novel tannase enzyme present in some *Lactobacillus plantarum* strains. Appl. Environ. Microbiol. 80 (10), 2991–2997.

Jurrus, E., Engel, D., Star, K., Monson, K., Brandi, J., Felberg, L.E., Brookes, D.H., Wilson, L., Chen, J., Liles, K., Chun, M., 2018. Improvements to the APBS biomolecular solvation software suite. Proteome Sci. 27, 112–128.

Kanpiengjai, A., Khanongnuch, C., Lumyong, S., Haltrich, D., Nguyen, T., Kittibunchakul, S., 2020. Co-production of gallic acid and a novel cell-associated tannase by a pigment-producing yeast, *Sporidiobolus ruineniae* A45.2. Microb. Cell Fact. 19, 95.

Kanpiengjaia, A., Unban, K., Nguyen, T., Haltrichc, D., Khanongnuch, C., 2019. Expression and biochemical characterization of a new alkaline tannase from Lactobacillus pentosus. Protein Expr. Purif. 157, 36–41.

Kar, B., Banerjee, R., 2000. Biosynthesis of tannin acyl hydrolase from tannin-rich forest residue under different fermentation conditions. J. Ind. Microbiol. Biotechnol. 25, 29–38.

Kaur, G., Pati, P.K., 2018. In silico physicochemical characterization and topology analysis of respiratory burst oxidase homolog (Rboh) proteins from Arabidopsis and rice. Bioinformation 14, 93–100.

Kikuchi, Y., Ohbayashi, T., Jang, S., Mergaert, P., 2020. Burkholderia insecticola triggers midgut closure in the bean bug Riptortus pedestris to prevent secondary bacterial infections of midgut crypts. ISME J. 1–12.

Kiraga, J., Mackiewicz, P., Mackiewicz, D., Kowalczuk, M., Biecek, P., Polak, N., Smolarczyk, K., Dudek, M.R., Cebrat, S., 2007. The relationships between the

isoelectric point and: length of proteins, taxonomy and ecology of organisms. BMC Genom. 8, 163.
Kumar, S., Nussinov, R., 1999. Salt bridge stability in monomeric proteins. J. Mol. Biol. 293, 1241–1255.
Kuppan, G., Balasubramanyam, J., Monickaraj, F., Srinivasan, G., Mohan, V., Balasubramanyam, M., 2010. Transcriptional regulation of cytokines and oxidative stress by gallic acid in human THP-1 monocytes. Cytokine 49, 229–234.
Laskowski, R.A., MacArthur, M.W., Moss, D.S., Thornton, J.M., 1993. PROCHECK: a program to check the stereochemical quality of protein structures. J. Appl. Cryst. 26, 283–291.
Lewis, J.A., Starkey, R.L., 1969. Decomposition of plant tannins by some soil microorganisms. Soil Sci. 107, 235–241.
Lieutaud, P., Ferron, F., Uversky, A.V., Kurgan, L., Uversky, V.N., Longhi, S., 2016. How disordered is my protein and what is its disorder for? A guide through the "dark side" of the protein universe. Intrinsically Disord. Proteins 4, e1259708.
Maheshwari, B., Jain, A.K., 2019. Generalized seniority Schmidt model and the g-factors in semi-magic nuclei. Nucl. Phys. 986, 232–244.
Matsuda, M., Hirose, Y., Kanauchi, M., 2016. Purification and characteristics of tannase produced by lactic acid bacteria, *Lactobacillus plantarum* H78. J. Am. Soc. Brew. Chem. 74 (4), 258–266.
Mitra, D., Bandyopadhyay, A.K., Islam, R.N.U., Banerjee, S., Yasmeen, S., Mohapatra, P.K.D., 2019. November. Structure, salt-bridge's energetics and microenvironments of nucleoside diphosphate kinase from halophilic, thermophilic and mesophilic microbes. In: Biotechnology and Biological Sciences: Proceedings of the 3rd International Conference of Biotechnology and Biological Sciences (BIOSPECTRUM 2019), August 8-10, 2019. CRC Press, Kolkata, India, pp. 107–113.
Mohapatra, P.K.D., Mondal, K.C., Pati, B.R., 2005. Effect of inorganic constituents on growth and tannase production by Bacillus licheniformis KBR6. Ind. J. Biol. Sci. 70, 68–72.
Mohapatra, P.D., Mondal, K.C., Pati, B.R., 2006. Production of tannase through submerged fermentation of tannin-containing plant extracts by Bacillus licheniformis KBR6. J. Microbiol. 55, 297–301. PMID: 17416066.
Mohapatra, P.D., Pati, B.R., Mondal, K.C., 2009. Effect of amino acids on tannase biosynthesis by Bacillus licheniformis KBR6. J. Microbiol. Immunol. Infect. 42, 172–175. PMID: 19597651.
Mondal, K.C., Pati, B.R., 2000. Studies on the extracellular tannase from newly isolated Bacillus licheniformis KBR 6. J. Basic Microbiol. 40, 223–232.
Natarajan, K., Rajendran, A., 2012. Evaluation and optimization of food-grade tannin acyl hydrolase production by a probiotic Lactobacillus plantarum strain in submerged and solid state fermentation. Food Bioprod. Process. 90, 780–792.
Nayek, A., Gupta, P.S.S., Banerjee, S., Sur, V.P., Seth, P., Das, S., Islam, R.N.U., Bandyopadhyay, A.K., 2015. ADSBET2: automated determination of salt-bridge energy-terms version 2. Bioinformation 11, 413–415.
Nayek, A., Banerjee, S., Gupta, P., Sur, B., Seth, P., Das, S., Baker, N.A., Bandyopadhyay, A., 2015. ADSETMEAS: Automated determination of salt-bridge energy terms and micro environment from atomic structures using APBS method, version 1.0. Protein Sci. 2016–2017.
Panda, S., Chandra, G., 2012. Physicochemical characterization and functional analysis of some snake venom toxin proteins and related non-toxin proteins of other chordates. Bioinformation 8, 891–896.
Patil, D.B., Das, S.K., Das Mohapatra, P.K., Nag, A., 2011. Physico-chemical studies and optimization of gallic acid production from the seed coat of Terminalia belerica Roxb. Ann. Microbiol. 61, 649–654.
Pauleta, S.R., Lu, Y., Goodhew, C.F., Moura, I., Pettigrew, G.W., Shelnutt, J.A., 2001. Calcium-dependent conformation of a heme and fingerprint peptide of the diheme cytochrome c peroxidase from Paracoccus pantotrophus. Biochemistry 40, 6570–6579.
Podschun, R., Ullmann, U., 1998. Klebsiella spp. as nosocomial pathogens: epidemiology, taxonomy, typing methods, and pathogenicity factors. Clin. Microbiol. Rev. 11, 589–603.
Qin, S., Xing, K., Jiang, J.H., Xu, L.H., Li, W.J., 2011. Biodiversity, bioactive natural products and biotechnological potential of plant-associated endophytic actinobacteria. Appl. Microbiol. Biotechnol. 89, 457–473.
Raghuwanshi, S., Dutt, K., Gupta, P., Misra, S., Saxena, R.K., 2011. Bacillus sphaericus: the highest bacterial tannase producer with potential for gallic acid synthesis. J. Biosci. Bioeng. 111, 635–640.
Rambaut, A., 2014. Figtree, a Graphical Viewer of Phylogenetic Trees [Internet].
Ren, B., Wu, M., Wang, Q., Peng, X., Wen, H., McKinstry, W.J., Chen, Q., 2013. Crystal structure of tannase from Lactobacillus plantarum. J. Mol. Biol. 425, 2737–2751.
Rigoldi, F., Donini, S., Redaelli, A., Parisini, E., Gautieri, A., 2018. Engineering of thermostable enzymes for industrial applications. APL Bioeng 2, 011501.
Rodriguez, H., Rivas, B., Gomez-Cordoves, C., Munoz, R., 2008. Characterization of tannase activity in cell-free extracts of Lactobacillus plantarum CECT 748T. Int. J. Food Microbiol. 121, 92–98.
Schröder, C., 2017. Proteins in ionic liquids: current status of experiments and simulations. In: Ionic Liquids II. Springer, Cham, pp. 127–152. PMID: 28176271.
Schröttner, P., Rudolph, W.W., Taube, F., Gunzer, F., 2014. First report on the isolation of Aureimonas altamirensis from a patient with peritonitis. Int. J. Infect. Dis. 29, 71–73.
Sharma, S., Agarwal, L., Saxena, R.K., 2007. Statistical optimization for tannase production from Aspergillus Niger under submerged fermentation. Indian J. Microbiol. 47, 132–138.
Sievers, F., Wilm, A., Dineen, D., Gibson, T.J., Karplus, K., Li, W., Lopez, R., McWilliam, H., Remmert, M., Söding, J., Thompson, J.D., 2011. Fast, scalable generation of high-quality protein multiple sequence alignments using Clustal Omega. Mol. Syst. Biol. 7, 1–6.
Thiyonila, B., Kannan, M., Reneeta, N.P., Ramya, T., Kayalvizhi, N., Krishnan, M., 2020. Influence of tannase from Serratia marcescens strain IMBL5 on enhancing antioxidant properties of green tea. Biocatal. Agric. Biotechnol. 101675.
Tretyachenko, V., Vymětal, J., Bednárová, L., Kopecký, V., Hofbauerová, K., Jindrová, H., Hubálek, M., Souček, R., Konvalinka, J., Vondrášek, J., Hlouchová, K., 2017. Random protein sequences can form defined secondary structures and are well-tolerated in vivo. Sci. Rep. 7, 1–9.
Ueda, S., Nomoto, R., Yoshida, K., Osawa, R., 2014. Comparison of three tannases cloned from closely related lactobacillus species: *L. Plantarum, L. Paraplantarum, and L. Pentosus*. BMC Microbiol. 14 (87), 1–9, 2014. http://www.biomedcentral.com/1471-2180/14/87.
Unban, K., Kodchasee, P., Shetty, K., Khanongnuch, C., 2020. Tannin-tolerant and extracellular tannase producing Bacillus isolated from traditional fermented tea leaves and their probiotic functional properties. Foods 9, 490.
UniProt Consortium, 2015. UniProt: a hub for protein information. Nucleic Acids Res. 43, D204–D212.
Yadav, A.N., Verma, P., Kumar, S., Kumar, V., Kumar, M., Sugitha, T.C.K., Singh, B.P., Saxena, A.K., Dhaliwal, H.S., 2018. Actinobacteria from rhizosphere: molecular diversity, distributions, and potential biotechnological applications. In: New and Future Developments in Microbial Biotechnology and Bioengineering. Elsevier, pp. 13–41.
Zhang, Z., Lu, Y., Chi, Z., Liu, G., Jiang, H., Hu, Z., Chi, Z., 2019. Genome editing of different strains of Aureobasidium melanogenum using an efficient Cre/loxp site-specific recombination system. Fung. Biol. 123, 723–731.